Bacterial SOS Genes *mucAB/umuDC* Promote Mouse Tumors by Activating Oncogenes *Nedd9/Aurkb* via a miR-145 Sponge

Hiroshi Tanooka[1,2,3], Ayako Inoue[1], Ryou-u Takahashi[1], Kouichi Tatsumi[3], Kazuo Fujikawa[4], Tetsuji Nagao[4], Masamichi Ishiai[2], Fumiko Chiwaki[5], Kazuhiko Aoyagi[5], Hiroki Sasaki[5], and Takahiro Ochiya[1,6]

ABSTRACT

The mechanism of cancer induction involves an aberrant expression of oncogenes whose functions can be controlled by RNAi with miRNA. Even foreign bacterial RNA may interfere with the expression of oncogenes. Here we show that bacterial plasmid *mucAB* and its *Escherichia coli* genomic homolog *umuDC,* carrying homologies that match the mouse anti-miR-145, sequestered the miR-145 function in mouse BALB 3T3 cells in a tetracycline (Tet)-inducible manner, activated oncogene *Nedd9* and its downstream *Aurkb,* and further enhanced microcolony formation and cellular transformation as well as the short fragments of the bacterial gene containing the anti-miR-145 sequence. Furthermore, *mucAB* transgenic mice showed a 1.7-fold elevated tumor incidence compared with wild-type mice after treatments with 3-methylcolanthrene. However, the mutation frequency in intestinal stem cells of the *mucAB* transgenic mice was unchanged after treatment with X-rays or ethyl-nitrosourea, indicating that the target of *mucAB/umuDC* is the promotion stage in carcinogenesis.

Implications: Foreign bacterial genes can exert oncogenic activity via RNAi, if endogenously expressed.

Visual Overview: http://mcr.aacrjournals.org/content/molcanres/18/9/1271/F1.large.jpg.

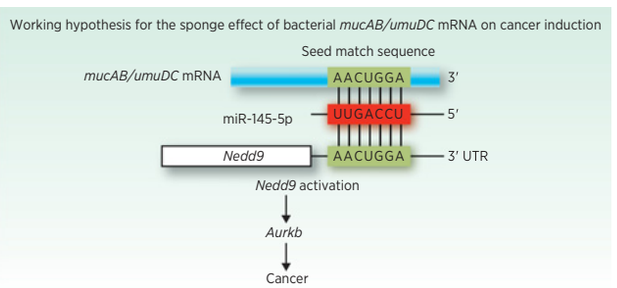

Introduction

RNAi is a key mechanism for controlling biological functions (1). miRNAs regulate the expression of a number of oncogenes via interaction with their messenger RNAs (mRNA) at the seed sequence of the untranslated region (UTR; refs. 2, 3). Their interference leads to uncontrolled cell growth and thus to cancer (4). Among a variety of interfering RNA species, endogenously expressed competitive RNA exerts a sponge effect to sequester the function of miRNA (5). Specifically, RNA transcribed from the pseudogene of the human tumor suppressor *PTEN* controls parental *PTEN* expression by interacting with miRNA (6) and, further, human *TYRP1* mRNA interferes with the tumor suppressor miR-16, rendering cells cancerous (7). In this context, even endogenously expressed foreign RNA from the bacterial origin may exert a sponge effect to cause a cancer.

This study was initially undertaken to examine the role of the error-prone DNA repair mechanism accompanied by the SOS response of cells (8, 9) in cancer induction with a bacterial error-prone gene, because mutagenesis is thought to be an important step in carcinogenesis. Previously, enterobacterial plasmid gene *mucAB* (10) that serves the SOS function, rescuing cell survival by sacrificing DNA repair fidelity via translesion DNA synthesis (11), was found to transform mouse BALB 3T3 cells after endogenous expression without forming MucB proteins (12). The mechanism underlying this apparently strange phenomenon, however, has been unclear. We show here that *mucAB* and its *Escherichia coli (E. coli)* genomic homolog *umuDC* (13), when expressed in mouse BALB 3T3 cells, interact with miR-145, a tumor suppressor (14, 15), activate oncogene *Nedd9* under control of miR-145 (15, 16) and its downregulated oncogene *Aurkb* (17, 18). Observation was further extended to examine these effects on cellular transformation of mouse cells and tumor induction in the mouse whole body system.

Materials and Methods

Construction of plasmids with expression vectors

Full lengths of *mucAB* and *umuDC* (**Fig. 1**; Supplementary Fig. S1) were inserted into Tet-inducible vector pcDNA4/TO (Invitrogen),

[1]Division of Molecular and Cellular Medicine, National Cancer Center Research Institute, Tokyo, Japan. [2]Central Radioisotope Division, National Cancer Center Research Institute, Tokyo, Japan. [3]Biological Effects Research Group, Research Center for Radiation Protection, National Institute of Radiological Sciences, Chiba, Japan. [4]Department of Life Science, Faculty of Science and Technology, Kindai University, Higashiosaka, Japan. [5]Department of Translational Oncology, National Cancer Center Research Institute, Tokyo, Japan. [6]Department of Molecular and Cellular Medicine, Tokyo Medical University, Tokyo, Japan.

Note: Supplementary data for this article are available at Molecular Cancer Research Online (http://mcr.aacrjournals.org/).

Current address for R. Takahashi: Department of Cellular and Molecular Biology, School of Pharmaceutical Sciences, Graduate School of Biomedical & Health Sciences, Hiroshima University.

Corresponding Author: Hiroshi Tanooka, National Cancer Center, 5-1-1 Tsukiji, Chuo-ku, Tokyo 104-0045, Japan. Phone: 813-3542-2511; Fax: 813-542-0623; E-mail: tanooka-h@wind.ocn.ne.jp

Mol Cancer Res 2020;18:1271–7

doi: 10.1158/1541-7786.MCR-20-0137

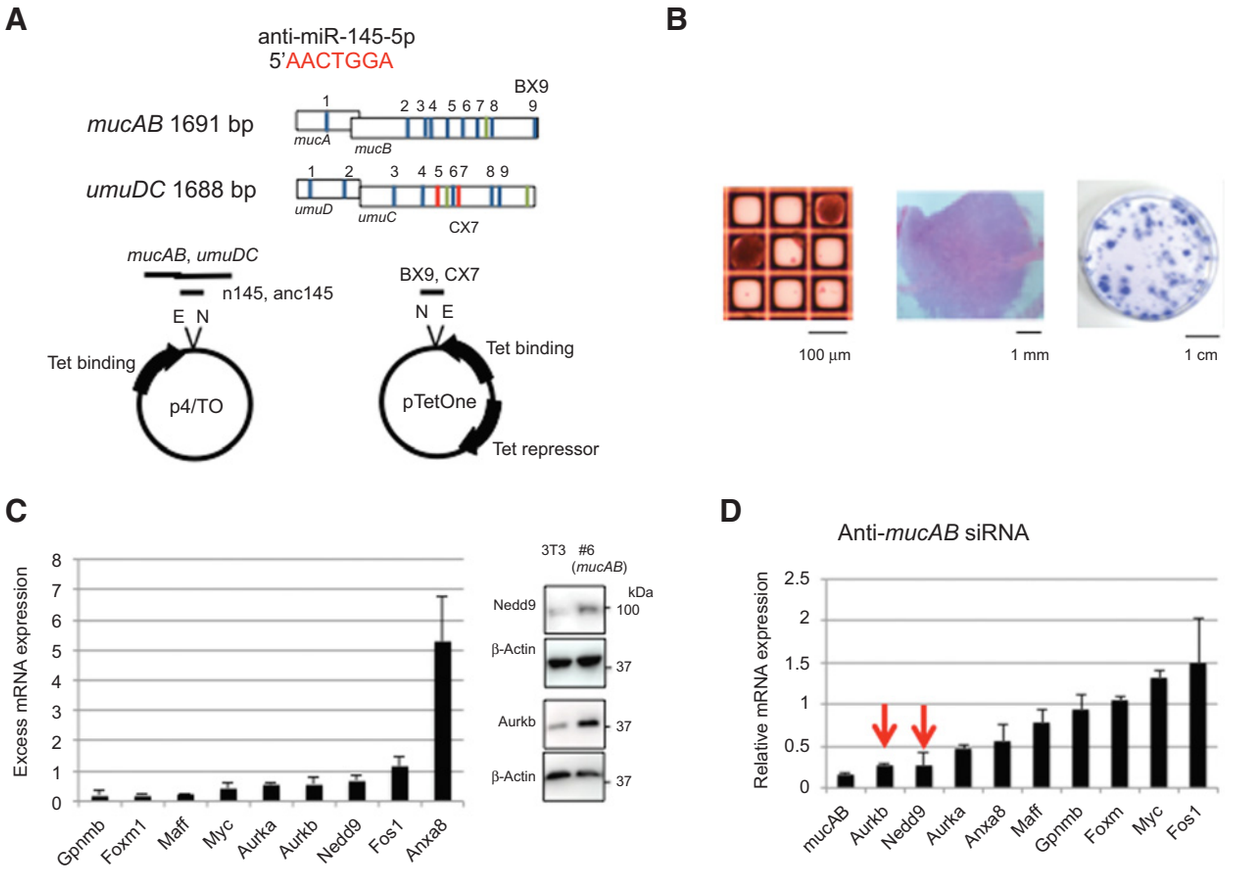

Figure 1.

Search for the target oncogene of *mucAB*. **A,** *mucAB* and *umuDC* open reading frames showing the *Nedd9* seed match (anti-miR-145-5p) sequences (blue bar: 5 ntd match; red bar: 7 ntd match. BX9: 9th homology in *mucAB*. CX7: 7th homology in *umuDC*) and *Aurkb* seed match (anti-miR-466-3p) sequences (green bar: 5 ntd match). Nucleotide sequences of full-length of *mucAB* and *umuDC* are shown in Supplementary Fig. S1. Tet-inducible expression vectors, pcDNA 4/TO with insert: *mucAB* or *umuDC*, positive control n145 with anti-miR-145, or negative control anc145 (Supplementary Table S1), and pcDNA TetOne with insert: BX9 or CX7, short fragments of *mucAB* or *umuDC* with the anti-miR-145-5p. E, *Eco*RI; N, *Not*I. **B,** Left, microwells showing microcolonies grown from single N11 cells (filled box) and cells that remained quiescent after Tet induction; histologic section of a tumor formed after transplantation of N11 cells expanded from a microcolony into a SCID mouse; and foci of N11 cells transformed with Tet. **C,** Oncogene mRNAs increased in the transformable #6 cells (*mucAB*$^{+}$), compared with control BALB 3T3 cells, as measured by qPCR (left) and Western blotting analysis of Nedd9 and Aurkb proteins in #6 cells compared with BALB 3T3 cells (right). **D,** Suppressive effects of anti-*mucAB* siRNA (mmucAB#1) on oncogene mRNA expressions in #6 cells, as measured by qPCR. Expression levels were normalized to the untreated #6 cell levels. Arrows show highest suppressions to *Aurkb* and *Nedd9*. Quantification: $n = 3$ biological replicas.

respectively. Synthetic short-length inserts (Supplementary Table S1) were n145 that carries the anti-miR-145-5p sequence plus 10-bp flanking sequences, its negative control anc145 with the reversed sequence, and BX9 and CX7 that are portions of *mucAB* and *umuDC*, each containing the anti-miR-145 sequence. n145 and anc145 were inserted into p4/TO and BX9 and CX7 were inserted into pTetOne (Invitrogen). Constructs were confirmed by gel electrophoresis for restriction sites and by direct sequencing. Plasmids were amplified in *E. coli* HB101 DH5α (TOYOBO) grown in an LB medium containing 100 µg/mL ampicillin (Sigma-Aldrich) and extracted using a Wizard Kit (Promega).

Cell lines

The mouse cell line BALB 3T3 was originally obtained from ATCC, cultured in DMEM (GIBCO), supplemented with 10% FCS (GIBCO) and 1% antibiotic–antimycotic (Life Technologies) at 37°C in a humidified CO_2 incubator, stored in a cell banker at liquid nitrogen temperature, and used for experiment within 10 passages after each thawing. Cells were not tested for *Mycoplasma*. Authentification was conducted for the absence of spontaneous transformation and the transformation with genotoxic agents. The derivative cell lines were treated in the same way. A cell line T212 that highly expressed the Tet repressor (Supplementary Fig. S2) was the host of 4/TO plasmids, while BALB 3T3 was the host of TetOne plasmids. Plasmids were introduced into cells using Lipofectamine LTX (Invitrogen) and selected in the medium containing 100 µg/mL zeocin and 10 µg/mL blastidicin for 4/TO, or 3.5 µg/mL puromycin for TetOne. Representative cell lines are N11 (n145/4TO/T212), NC41 (anc145/4TO/T212), AB-33 (*mucAB*/4TO/T212), DC-5 (*umuDC*/4TO/T212), BX9-615 (BX9/TetOne/3T3), and CX7-611 (CX7/TetOne/3T3). pTE40 with *mucAB* (12) was introduced into BALB 3T3 cells by cotransfection with pEGFp-N1 (Clontech) with LTX and selected in DMEM containing 400 µg/mL geneticin (Life Technologies) to yield cell line #6.

Treatment of cells and assay for gene expression

Locked nucleic acid (LNA, Mmu anti-miR-145a-5p; Qiagen) or negative control LNA-A (Qiagen) was introduced into cells at 20 nmol/L using lipofectamine 3000 (Life Technologies). siRNAs (Supplementary Table S1) were introduced into cells with DharmFECT (Thermo Fisher Scientific) at 100 nmol/L. For Tet induction, cells were treated in a DMEM-FCS medium supplemented with 1 μg/mL Tet for 2 days at 37°C. RNA was extracted using the miRNeasy Mini Kit (Qiagen) and converted to cDNA using the High-Capacity Reverse Transcription Kit (Applied Biosystems). PCR and qPCR were performed by GeneAmp (Applied Biosystems) and Real Time PCR 7300 (Applied Biosytems) using respective primers and probes (Supplementary Table S1). Products were further analyzed by electrophoresis on a 1% agarose gel.

Luminescence reporter

The fragments n145 and negative control anc145 were inserted into pmiRGLO-dual-luciferase miR target expression vector (Promega), yielding a reporter plasmid pG145 and pAG145, respectively. Reporters were introduced into cells using lipofectamine L3000. Cells lysates dissolved in M-PER (Thermo Fisher Scientific) were measured for luminescence using Dual-Glo Luciferase Assay System (Promega) with a Glo Max reader (Promega). A ratio of the firefly to the *Renilla* luminescence intensity (F/R) was taken as a measure of the miR-145 level.

Western blot analysis

Cells and tissues were homogenized in RIPA buffer (Sigma) supplemented with 1% proteinase inhibitor. Ten μg proteins were applied to electrophoresis on a 4% to 20% PAGE gel and transferred to a polyvinylidene difluoride membrane. The membranes were treated in a blocking buffer with antibodies for rabbit Aurkb (ab2254, Abcam) or mouse Nedd9 (4044, Cell Signaling Technology), and then with horseradish peroxidase–conjugated anti-rabbit IgG (P0360, DAKO) or anti-mouse IgG (DAKO), respectively. Proteins were detected using Western blotting substrates (Thermo Fisher Scientific) and a FUSION chemiluminescence imaging system (Vilber-Lourmat).

Microcolonies

Micro-Space Cell Culture Plate (Elplasia, KURARAY) consists of 12 wells (1 cm in diameter), each carrying microwells (size: width 100 μm, height 100 μm; **Fig. 1B**). Cells grown in a DMEM-FCS medium were filtered through a membrane (FALCON), suspended at 4×10^3 cells/mL, and 1 mL was plated in a well. This method ensures that each microwell contains a single cell. After incubation for 20 days at 37°C, the number of wells with a single cell (A) or with multiple cells (B) was counted under a microscope. The ratio B/(A+B) was taken as a measure of microcolony frequency. Microcolonies were further expanded and transplanted to SCID mice (Charles River Laboratories, Japan) for tumor formation (**Fig. 1B**).

Cell transformation

Cells grown to the semiconfluent stage in DMEM-FCS were plated at 2×10^5 cells per dish in the same medium with or without 1 μg/mL Tet and followed for formation of foci with weekly medium changes for 5 weeks. Cells were then washed with PBS, fixed with methanol, stained with 10% Gimsa stain solution (Sigma-Aldrich), and counted for the number of foci of transformed cells (**Fig. 1B**). Cells expanded from the foci were further transplanted into SCID mice.

Transgenic mice with *mucAB* and tumor induction

The 5.5 kbp *Eco*RI-digested fragments of pTE 40 (12) containing *mucAB* were introduced into C57BL/6J mouse embryos at Oriental Yeast Co., Japan. From 223 embryos embedded, 38 mice were born and one heterozygous male with *mucAB* was obtained, after screening of tail DNA with PCR and 1% gel electrophoresis. This male was cross-bred with wild-type female mice to obtain heterozygous $mucAB^{+/-}$ mice, which were further cross-bred to obtain homozygous $mucAB^{+/+}$mice. The mice were registered as C57BL/6J-Tg(pTE40) Nrs, and frozen embryos were preserved at the Riken BioResource Center (Japan).

Tumors were induced by subcutaneous injection of 0.1 mL of 0.2 mg/mL 3-methylcolanthrene (3-MC; Sigma-Aldrich) dissolved in olive oil at the groin at 8 weeks of age, so as to give a median tumor incidence rate in wild-type mice (19), and observed weekly for their formation for 400 days. The day of tumor appearance was defined as the day when a tumor reached a diameter of 3 mm. When the tumor was found at a larger size, this date was calculated by extrapolation assuming 2.6 days for tumor volume doubling time (19). Tumors were sectioned, fixed with 10% formalin, stained with haematoxylin and eosin, and examined histologically under a microscope.

Mutation assay in mouse intestinal stem cells

The homozygous $mucAB^{+/+}$ transgenic mice were crossed with mutant SWR mice with a clonal marker $Dlb\text{-}1^a$ (ref. 20; The Jackson Laboratory) to yield heterozygous $Dlb\text{-}1^b/Dlb\text{-}1^a$ F_1 mice. The *Dlb* locus determines the expression of binding sites for the lectin Dolichos biflorus agglutinin (DBA) in intestinal epithelium. The mice were treated at 8 weeks of age with 140 kVp X-rays at a dose rate of 0.5 Gy/minute or intraperitoneal injection of ethylnitrosourea (ENU; Sigma-Aldrich) dissolved in PBS, and sacrificed after 2 weeks. The small intestine was stained with a lectin DBA-peroxidase conjugate (Wako Pure Chemicals). Villi with mutations at the *Dlb-1* locus were detected as a white nonstaining ribbon and were counted for 10,000–11,000 per mouse.

Statistical analysis

All quantitative values are presented as mean ± SD. Significance of differences in means was tested by the *t* test. A probability value of less than 0.05 was considered statistically significant.

Data availability

All data are available from the corresponding author. Microarray data have been deposited in the NCBI Genome Expression Omnibus (GEO) under the accession code GSE84896.

Ethics approval

Recombination and animal experiments were performed under the guidelines after approval of the ethics committee of the respective institution: National Cancer Center Research Institute, National Institute of Radiological Science, and Kindai University.

Results

Search for target gene

We noted the presence of nucleotide sequences in *mucAB* and *umuDC* that are homologous to the seed sequence at the 3′UTR of mRNA of the mouse oncogene *Nedd9* (**Fig. 1A**; Supplementary Fig. S1). This sequence matches mmu-miR-145a-5p complementarily and is expected to interact with miR-145 as an anti-miR-145 in mouse cells. Furthermore, the *Nedd9* seed match sequence is more abundant than the *Aurkb* seed match sequence (anti-miR-466-3p) in both of

mucAB and *umuDC* (number of *Nedd9* seed matches: 9 in *mucAB* and 9 in *umuDC*; number of *Aurkb* seed matches: 1 in *mucAB* and 2 in *umuDC*). This abundance indicates that *Nedd9* interacts with *mucAB*/*umuDC* more efficiently than *Aurkb*.

A microarray search provided 126 deregulated genes in transformation-positive #6 cells, compared with transformation-negtive BALB 3T3 cells. From these genes, 10 oncogenes were selected (Supplementary Fig. S3). The upregulated oncogenes were confirmed for their mRNA expression by qPCR (**Fig. 1C**, left). *Nedd9* was added here because *Nedd9* controls expression of the important candidate *Aurkb*, while *Nedd9* expression was under the detection level of microarray. Nedd9 and Aurkb proteins were also increased in #6 cells, compared with BALB 3T3 cells (**Fig. 1C**, right). The candidate oncogenes were further examined for their mRNA expression changes in response to anti-*mucAB* siRNA (Supplementary Table S1) in #6 cells, showing highest suppression in *Aurkb* and *Nedd9* (**Fig. 1D**). In parallel, anti-*mucAB* shRNA suppressed transformation of #6 cells (Supplementary Fig. S4).

Accordingly, we propose a working hypothesis that mRNAs of *mucAB*/*umuDC* competitively interfere with miR-145, which controls expression of *Nedd9* and its downstream *Aurkb*, leading to cancer (visual overview).

Anti-miR-145 elevates *Nedd9* and *Aurkb* expressions, microcolony formation, and cellular transformation

The effect of anti-miR-145 LNA on the miR-145 level was confirmed by the reporter pG145 (**Fig. 2A**). The luminescence of the empty pmiRGLO was lowered by the presence of anti-miR-145. This lowering was restored by anti-miR-145 LNA. At the same time, *Nedd9* and *Aurkb* mRNA expressions were elevated, indicating that the miR-145 level controls the expression of *Nedd9* and its downstream *Aurkb*.

As a further positive control, N11 cells with the Tet-inducible anti-miR-145 were examined (**Fig. 2A**). First, Tet-induction increased the luminescence of the reporter pG145. In a reverse way, Tet-treatment of N11 cells decreased the luminescence of

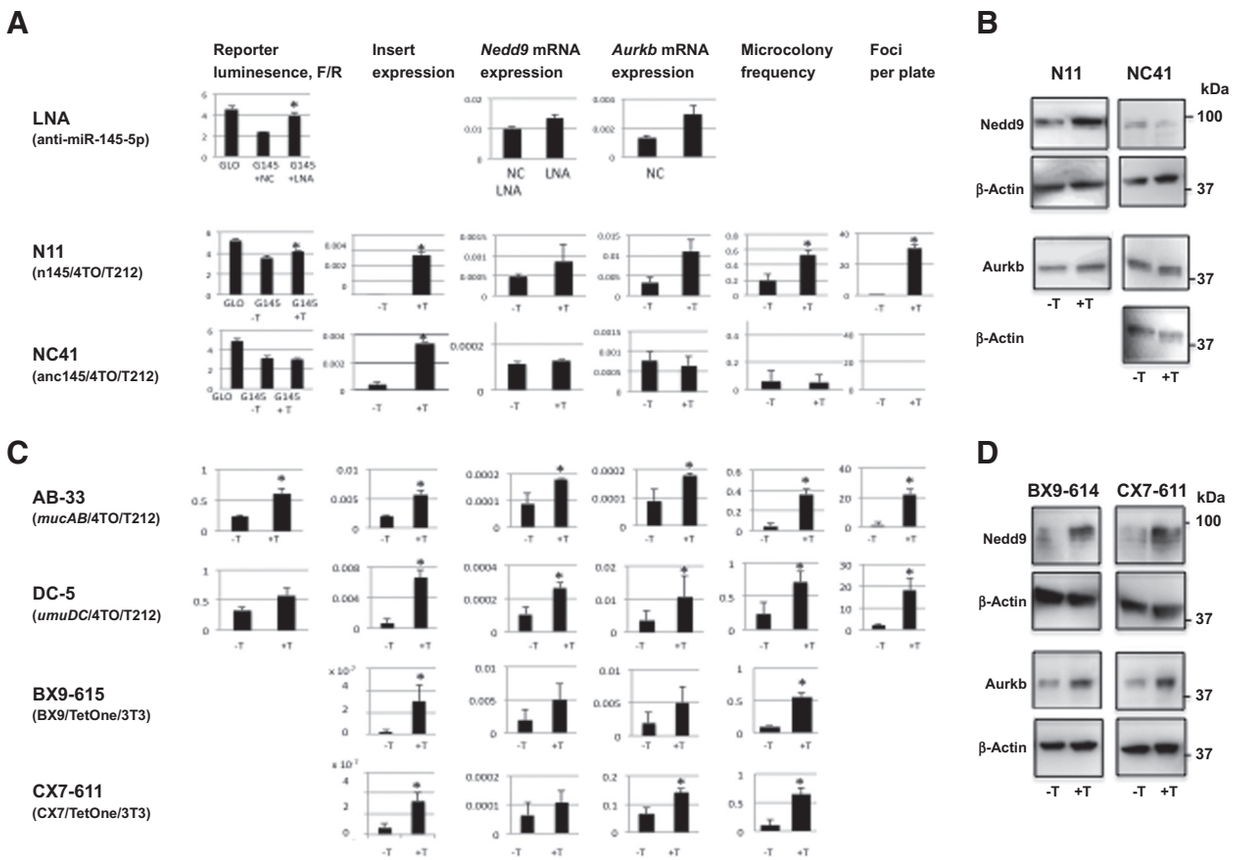

Figure 2.

Cellular response to Tet-induction of anti-miR-145, *mucAB,* and *umuDC*. **A,** Effects of LNA (anti-miR-145-5p) on luminescence of the miR-145 reporter pG145 and the expression of *Nedd9* and *Aurka* mRNAs in BALB 3T3 cells; GLO: empty reporter; NC: negative control LNA. Effect of Tet-induction on N11 cells carrying the insert n145 (anti-miR-145) on the reporter luminescence, expression of RNA from the insert, expression of *Nedd9* and *Aurkb* mRNAs, microcolony formation, and foci formation (from left to right). NC41: negative control cells with insert anc145. Foci were absent with or without Tet. **B,** Nedd9, Aurkb, and β-actin proteins in N11 and NC41 cells after treated with or without Tet, as measured by Western blotting analysis. **C,** Effects of Tet-induction of AB-33(*mucAB*), DC-5(*umuDC*), BX9-615, and CX7-611 cells on the reporter luminescence, expression of RNA from the insert, expression of *Nedd9* and *Aurkb* mRNAs, microcolony formation, and foci formation (from left to right). **D,** Nedd9, Aurkb, and β-actin proteins in BX9-615 and CX7-611 cells after treated with or without Tet, as measured by Western blotting analysis. Quantification: $n = 4$ biological replicas for reporter assay and $n = 3$ for others. *, statistically significant increase by Tet induction ($P < 0.05$).

pAG145 (Supplementary Fig. S5). These control experiments show that the expressed RNA of a short length, consisting of the vector-origin RNA (220 ntd) and RNA from the insert (30 ntd), can act for RNAi. Furthermore, Tet-treatment of N11 cells enhanced *Nedd9* and *Aurkb* mRNA levels together with formation of microcolonies from single cells plated in microwells and formation of foci from transformed cells. Negative control NC 41 cells did not show these effects. Furthermore, Tet-treatment of N11 cells increased Nedd9 and Aukb proteins to a certain extent, while this increase was absent in negative control NC41 cells (**Fig. 2B**, right). The above findings indicate that anti-miR-145 interacts with cellular miR-145 that control expression of *Nedd9* and its downstream *Aurkb*, leading to cellular transformation.

To confirm the validity of the microcolony test, a time course was followed for single N11 cells seeded in microwells (Supplementary Fig. S6), showing a distinct difference between Tet-treated and untreated cells. Tumors from transplants of microcolonies were histologically fibrosarcomas (**Fig. 1B**): 9 transplantable of 12 microcolonies, compared with 8 transplantable of 12 foci. BALB 3T3 cells did not produce tumors. Therefore, cells grown to the microcolony stage seemed to be already committed to the tumorigenesis process.

mucAB/umuDC elevates *Nedd9* and *Aurkb* expressions, microcolony formation, and cellular transformation

Full lengths of *mucAB* and *umuD* were then examined for their effects on cellular responses upon Tet-induced expression. Representative cell lines, AB-33 and DC-5, showed the increase of luminescence of the reporter upon Tet-induction of *mucAB* and *umuDC* mRNAs, respectively (**Fig. 2C**, left). This indicates the interaction of *mucAB* and *umuDC* RNAs with miR-145. The Tet-induction further increased *Nedd9* and *Aurkb* mRNA expressions, together an increase of the frequency of microcolony formation and the frequency of foci. These observations were much the same as seen in positive control N11 cells.

These effects were further tested with a short fragment of *mucAB* or *umuDC* containing the anti-miR-145 sequence. Test cells were BX9-615 and CX7-611, in which the bacterial gene fragments BX9 and CX7 were respectively incorporated. Upon addition of Tet, these cells exhibited an increase of transcription of the insert, together with an increase of the expression of *Nedd9* and *Aurkb* mRNAs, and an increase of the frequency of microcolony formation (**Fig. 2C**). Nedd9 and Aurkb proteins were also increased by Tet treatment in BX9-615 and CX7-611cells (**Fig. 2D**). These results indicate that a portion of *mucAB* or *umuDC* with the anti-miR sequence can function for RNAi in mouse cells, exerting the oncogenic activity.

Transgene *mucAB* elevates tumor induction in mice

The study was further extended to the whole body system. The transgenic mice expressed full-length *mucAB* mRNA in the lung (**Fig. 3A**, left). The mice showed an increase of *Aurkb* mRNA expression in the lung and liver without Zn, compared with wild-type mice (**Fig. 3A**, right). The reason for the loss of metal dependence is unknown. No particular change in the phenotype or disorder was found in the transgenic mice.

Tumor formation was followed after subcutaneous injection of 3-MC over 400 days. Expression of *mucAB* was confirmed in tumors formed in the *mucAB* transgenic mice (**Fig. 3B**). The Kaplan–Meier plot for tumor formation showed a clear difference between *mucAB* transgenic and wild-type mice (**Fig. 3C**, left). Final tumor incidence was 55.4% for $mucAB^{+/+}$ (198 mice), 48.4% for $mucAB^{+/-}$ (97 mice), and 31.8% for wild-type mice (146 mice), that is, tumor incidence was 1.7-fold higher in total $mucAB^{+}$transgenic mice than in wild-type mice. There was no difference in tumor incidence rates between $mucAB^{+/+}$ and $mucAB^{+/-}$ mice (**Fig. 3C**), between males and females, or with and without Zn (Supplementary Fig. S7A and S7B). No tumors were formed in olive oil–injected mice (16 *mucAB* mice; 64 wild-type mice). Histologically, the majority of tumors were fibrosarcomas (95.1% of 182 total specimens examined), with rare rhabdomyosarcomas (3.2%) and squamous cell carcinomas (1.6%). The timing of when the tumor increase began was unchanged in the *mucAB* mice compared with wild-type mice. This indicates that *mucAB* exerts the oncogenic activity at the promotion stage of tumorigenesis.

Mutation frequency unchanged in intestinal stem cells of *mucAB* transgenic mice

A model system was $Dlb\text{-}1^{b}/Dlb\text{-}1^{a}$ F1 mice (20) with or without the *mucAB* transgene. The mice were treated with two doses of whole-body X-rays or ENU. No difference was found in the mutation frequency in the *Dlb-1* locus between $mucAB^{+}$ mice and control mice after each treatment (**Fig. 3D**). This indicates that oncomutation is not involved in the tumor-enhancing effect of *mucAB*.

Discussion

The present results showed that the enterobacterial SOS genes *mucAB* and *umuDC* carrying the anti-miR-145 seed sequence interfere with miR-145. In this case, the bacterial mRNAs may be included in the category of competitive endogenous RNA, as in the case of *PTEN* pseudogene transcripts and *TYRP1* mRNA. There might be a common underlying mechanism. The sponge effect is expected for these RNA interactions. However, the mechanism for processing these RNAs are not known and remained to be elucidated. Furthermore, it is interesting that the anti-miR signal is involved in the SOS function. The SOS function serves for adaptive response of cells to environmental change or genotoxic stress. It rescues cells from death, but on the other hand, creates mutation or even cancer and serves for evolution of the life. In this respect, the role of the anti-miR signal will become further important.

In this study, anti-miR-145 LNA activated expression of *Nedd9* and *Aurkb* RNAs by decreasing the cellular miR-145 level. Furthermore, N11 cells showed that the anti-miR-145 interfered with miR-145 and activated *Nedd9* and *Aurkb*. These observations show the interaction of miR-145 with the *Nedd9-Aurkb* pathway. Fragments of bacterial *mucAB* and *umuDC* with the anti-miR-145 sequence, BX9 and CX7, also exhibited the same effect. So did the whole *mucAB* and *umuDC*. These findings indicate that the anti-miR-145 interacts with miR-145, whatever its origin is bacteria or not.

Mouse BALB 3T3 cells are widely applied to the test of cellular transformation and are thought to be already committed to the initiation stage in the tumorigenesis steps because of their transformable character. Therefore, acceleration of the transformation by *mucAB/umuDC* accompanied by the activation of cell growth–related oncogenes *Need9/Aurkb* is thought to be related to the promotion step in tumorigenesis. Furthermore, in the mouse whole body, the timing of the start of tumor increase after treatment with a carcinogen 3-MC was unchanged, while the tumor incidence rate was elevated by the transgene *mucAB*. On the other hand, no increase of the mutation frequency was found in the intestinal stem cells of the *mucAB* transgenic mice. These findings indicate that oncomutation is not involved in the *mucAB* effect and that the

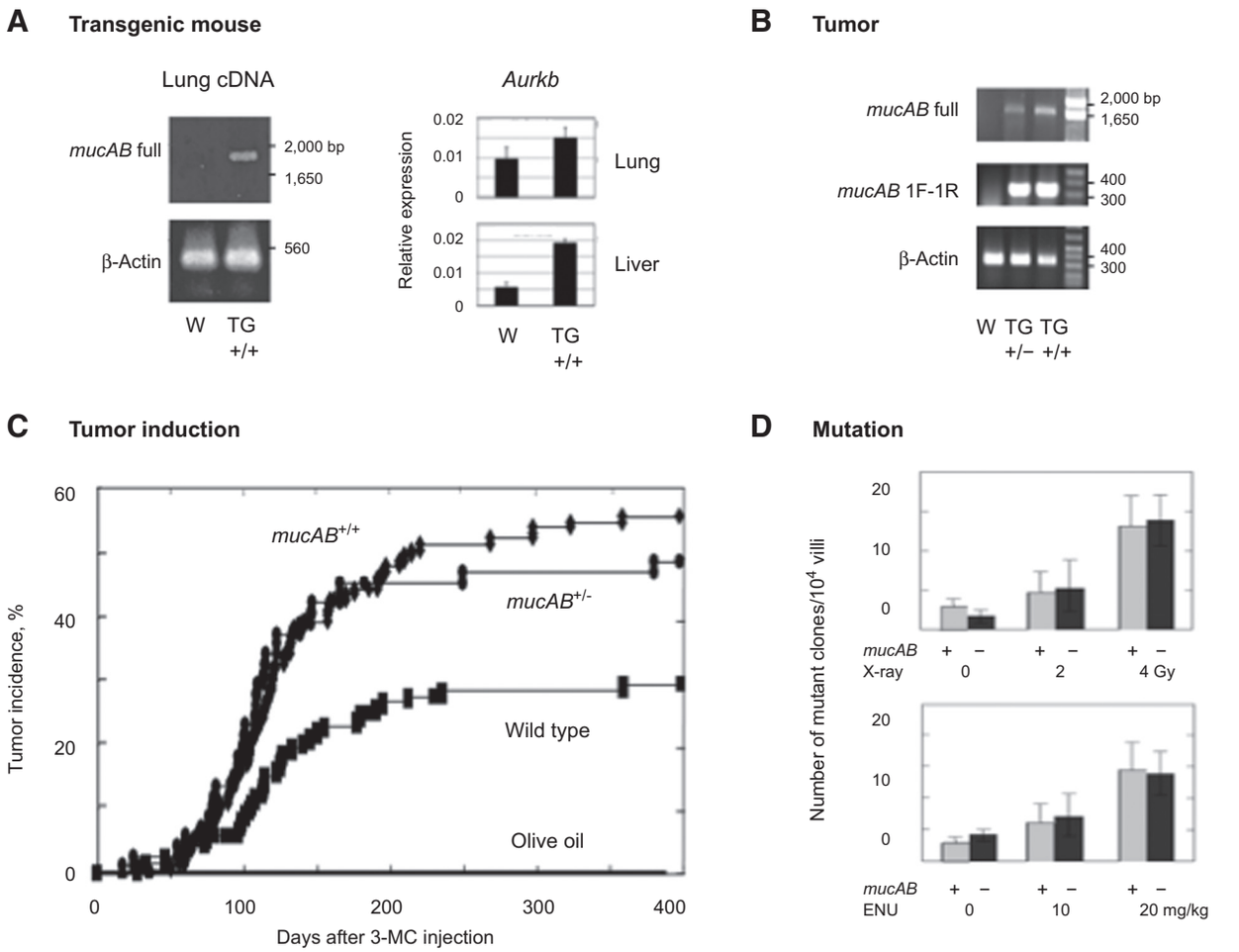

Figure 3.

Transgene *mucAB* promotes tumor formation in mice. **A,** Full-length *mucAB* mRNA expressed in the lung of $mucAB^{+/+}$ transgenic mouse (left) and expression of *Aurkb* mRNA in the lung and liver as measured by qPCR (right, $P < 0.05$, $n = 3$). W, wild-type; TG, transgenic. **B,** Expression of the *mucAB* transgene (full length and the 1F-1R portion) in a tumor produced by 3-MC. **C,** Kaplan–Meier plot for tumor induction after subcutaneous injection of 0.02 mg 3-MC at the groin of mice. The difference in final tumor incidence rate between $mucAB^{+/+}$ and wild-type, or $mucAB^{+/-}$ and wild-type mice was statistically significant ($P < 0.05$). The difference between $mucAB^{+/+}$ and $mucAB^{+/-}$ was statistically not significant ($P > 0.05$). **D,** Mutation frequency at the *dlb-1* locus in intestinal stem cells of heterozygous $Dlb\text{-}1^{a}/Dlb\text{-}1^{b}$ mice with or without the *mucAB* transgene after treatment with X-rays (top) or with ENU (bottom). ENU dose: mg/kg body weight. The differences in mutation frequency between $mucAB^{+}$ and $mucAB^{-}$ mice were statistically not significant ($P > 0.05$, $n = 4$).

promotion stage is the target of *mucAB*. Finally, involvement of enterobacterial genes in the cause of human gastric cancers is an interesting problem. However, we have no evidence for the presence of *mucAB/umuDC* homology in the genome of human cancers at present. Search on this will be continued in the future.

In conclusion, the present results provided an evidence that even foreign bacterial genes interfere with the function of miRNA as a sponge and promote tumors, when endogenously expressed.

Disclosure of Potential Conflicts of Interest

No potential conflicts of interest were disclosed.

Authors' Contributions

H. Tanooka: Conceptualization, resources, data curation, software, formal analysis, supervision, funding acquisition, validation, investigation, visualization, methodology, writing-original draft, project administration, writing-review and editing. **A. Inoue:** Investigation, methodology. **R. Takahashi:** Data curation, investigation, methodology. **K. Tatsumi:** Data curation, investigation, project administration. **K. Fujikawa:** Data curation, methodology. **T. Nagao:** Data curation, methodology. **M. Ishiai:** Formal analysis, validation, methodology. **F. Chiwaki:** Data curation, software, methodology. **K. Aoyagi:** Data curation, formal analysis, methodology. **H. Sasaki:** Data curation, formal analysis, investigation, methodology. **T. Ochiya:** Resources, data curation, supervision, funding acquisition, validation, investigation, project administration.

Acknowledgments

We thank T. Kato and K. Wakabayashi for the gifts of plasmids, K. Shimotohno, G. Fujii, and N. Tsuchiya for useful discussions, T. Kohno for advice on the Tet repressor, S. Kito and Y. Oota for preparing frozen mouse embryos, Y. Noda and H. Ishii-Ohba for support in animal experiments, T. Kawasaki and T. Iwai for animal care, T.S. Kuwata and Y. Nadatani for assistance in mouse mutation experiments, and members of the Division of Molecular and Cellular Medicine, National Cancer Center Research Institute and National Institute of Radiological Science for support of the work. This study was supported by Grants-in-aid for

Cancer Research, Ministry of Health and Welfare, Japan, and by Japan Agency for Medical Research and Development to T. Ochiya under grant number JP20cm0106402h0005.

The costs of publication of this article were defrayed in part by the payment of page charges. This article must therefore be hereby marked *advertisement* in accordance with 18 U.S.C. Section 1734 solely to indicate this fact.

Received February 10, 2020; revised March 31, 2020; accepted June 2, 2020; published first June 8, 2020.

References

1. Agrawal N, Dasaradhi PV, Mohmmed A, Malhotra P, Bhatnagar RK, Mukherjee SK. RNA interference: biology, mechanism, and applications. Microbiol Mol Biol Rev 2003;67:657–85.
2. Bartel DP. Micro RNAs: target recognition and regulatory functions. Cell 2009; 136:215–33.
3. Lai EC. Micro RNAs are complementary to 3′UTR sequence motifs that mediate negative post-translational regulation. Nat Genet 2002;30: 363–4.
4. Croce CM. Causes and consequences of microRNA dysregulation in cancer. Nat Rev Genet 2009;10:704–14.
5. Ebert MS, Neilson JR, Sharp PA. MicroRNA sponges: competitive inhibitors of small RNAs in mammalian cells. Nat Methods 2007;4:721–6.
6. Poliseno L, Salmena L, Zhang J, Carver B, Haveman WJ, Pandolfi PP. A coding-independent function of gene and pseudogene mRNAs regulates tumour biology. Nature 2010;465:1033–8.
7. Gilot D, Migault M, Bachelot L, Journé F, Rogiers A, Donnou-Fournet E, et al. A non-coding function of TYRP1 mRNA promotes melanoma growth. Nat Cell Biol 2017;19:1348–57.
8. Witkin EM. Ultraviolet mutagenesis and inducible DNA repair in Escherichia coli. Bacteriol Rev 1976;40:869–907.
9. Radman M. SOS repair hypothesis: phenomenology of an inducible DNA repair which is accompanied by mutagenesis. In: Hanawalt P, Setlow RB, editors. Molecular mechanisms for repair of DNA, part A. New York, NY: Plenum Publishing; 1970. p.355–67.
10. Perry KL, Elledge SJ, Mitchell BB, Marsh L, Walker GC. umuDC and mucAB operons whose products are required for UV light- and chemical-induced mutagenesis: UmuD, MucA, and LexA proteins share homology. Proc Natl Acad Sci U S A 1985;82:4331–5.
11. Sale JE, Lehman AR, Woodgate R. Y-family DNA polymerases and their role in tolerance of cellular DNA damage. Nat Rev Mol Cell Biol 2012;13:141–52.
12. Tosu M, Tanooka H. Transformation of mouse BALB 3T3 cells by enterobacterial plasmid misrepair gene mucAB. Mol Cell Biol 1990;10:5359–64.
13. Kitagawa Y, Akaboshi E, Shinagawa H, Hori T, Ogawa H, Kato T. Structural analysis of the umu operon required for inducible mutagenesis in Escherichia coli. Proc Nat Acad Sci U S A 1985;82:4336–40.
14. Gao P, Xing AY, Zhou GY, Zhang TG, Zhang JP, Gao C, et al. The molecular mechanism of microRNA-145 to suppress invasion-metastasis cascade in gastric cancer. Oncogene 2012;32,491–502.
15. Lu R, Ji Z, Li X, Zhai Q, Zhao C, Jiang Z, et al. miR-145 functions as tumor suppressor and targets two oncogenes, ANGPT2 and NEDD9, in renal cell carcinoma. J Cancer Res Clin Oncol 2014;140:387–97.
16. Speranza MC, Frattini V, Pisati F, Kapetis D, Porrati P, Eoli M, et al. Nedd9 as a novel target of miR-145, increases the invasiveness of glioblastoma. Oncotarget 2012;3:723–34.
17. Kozyreva VK, McLaughlin SL, Livengood RH, Calkins RA, Kelley LC, Rajulapati A, et al. NEDD9 regulates actin dynamics through cortactin deacetylation in an AURKA/HDAC6-dependent manner. Mol Cancer Res 2014;12:681–93.
18. Ice RJ, McLaughlin SL, Livengood RH, Culp MV, Eddy ER, Ivanov AV, et al. NEDD9 depletion destabilizes aurora A kinase and heightens the efficacy of aurora A inhibitors: implications for treatment of metastatic solid tumors. Cancer Res 2013;73:3168–80.
19. Tanooka H, Tanaka K, Arimoto H. Dose response and growth rates of subcutaneous tumors induced with 3-methylcholanthrene in mice and timing of tumor origin. Cancer Res 1982;42:4740–3.
20. Winton DJ, Blount MA, Ponder BAJ. A clonal marker induced by mutation in mouse intestinal epithelium. Nature 1988;333:463–6.